Earth Planets Space, **53**, 1065–1069, 2001

Power-law indices of asteroidal grooves and strength

Hirohide Demura

Lunar Mission Research Center, National Space Development Agency of Japan, Tsukuba Space Center, 2-1-1 Sengen, Tsukuba City, Ibaraki 305-8505, Japan

(Received January 12, 2001; Revised September 20, 2001; Accepted September 20, 2001)

The strength of an asteroid is a valuable parameter, but it is difficult to measure directly. Although impact experiments have made a large contribution, the problem of the relationship between an asteroid's size and its strength has not been solved. This paper introduces a valuable parameter for natural bodies, the power-law index ϕ of the size distribution of fracture planes [$N_S = k_S S^{-\frac{\phi}{2}}$]. This index can be regarded as parameterizing the strength, because strength is controlled by the size of the largest fracture. The power-law indices ϕ of the Martian satellite Phobos and the asteroid Gaspra were found to be 5.9 and 6.5, respectively. These values are close to 6, which is the theoretical value expected for the "fully cracked" condition of Housen and Holsapple (1999). The implications of this result for the size-strength relationship of asteroids are discussed.

1. Introduction

The destiny of small asteroids is controlled by their mechanical strength, since such bodies are severely damaged by impact processes during their evolution. We are interested in the destiny, lifetime and spatial distribution (as a function of size) of such objects, as such information will allow us both to reconstruct the history of the Solar System from the perspective of the origin of meteorites, and to cope with the threat of near-Earth objects. Although we do not have any means of measuring the strength of asteroids directly, we have known for some time that the density of flaws in a sample controls its static strength. Examples include the fracture mechanism of Griffith (1920), or Petch's law ($\sigma \propto d^{-\frac{1}{2}}$, where σ is the strength and d is a diameter of the body). However, there is no information in the literature on a measured power-law index of the fracture distribution of small irregular bodies. Strength, the upper limit of failure stress, is determined by the growth and coalescing of cracks. The growth of cracks is independent of size, because the growth rate is just the sound speed of the material, while coalescence is directly controlled by the cracks' spacing. In order to apply the results of impact experiments to natural bodies such as asteroids, we need to know the typical size and distribution of flaws, which gives the spacing. Here, I submit measurements of the power-law indices of the grooves of Phobos (the Martian satellite) and 951 Gaspra (an asteroid) as fundamental data for discussion of this issue.

The morphological unit that I use here, a groove, is a type of linear structure on the surface (Fig. 1). These bodies show unconnected chains of depressions, rather than obvious "grooves," but it is thought that these chains are open fractures covered by a regolith layer. Their typical dimensions are less than 10,000 m in length, less than 100 m in width, and ∼10 m in depth; they are commonly found on asteroids and small satellites such as Phobos (the Martian satellite), 951 Gaspra, 243 Ida, and 433 Eros (Table 1). An exception is the asteroid 253 Mathilde, on which no grooves have been reported. This may be due to its extremely low rigidity, which is inferred from its low density [1.3 g/cm^3] and similarity to primitive carbonaceous chondrites (as suggested from the C-type spectrum). In the case of Phobos, there are two competing models for the origin of the grooves: outcrops of internal fractures or superficial traces of impact craters (Fig. 2, right). Although some possible origins for internal fractures have been put forward, such as tidal stressing (Soter and Harris, 1977) and catastrophic impact (Veverka and Duxbury, 1977; Thomas *et al.*, 1978), laboratory experiments support the suggestion that the grooves originate directly from catastrophic impacts (Fujiwara and Asada, 1983; Kawakami *et al.*, 1991). The strongest support for this model comes from the observed similarity between the fracture patterns seen in impact experiments and the grooves of Phobos (Fig. 2, left).

2. Method

In this study, only the spacing of grooves was measured, because tracing the entire elongated structure of grooves on a small body is difficult. Spacing is defined with respect to a measured line on the surface of the body, and the spacing of intersections between the measured line and grooves is recorded. The two-dimensional (2D) size distribution of the grooves, and the corresponding three-dimensional (3D) distribution of fractures, are calculated. It should be noted that geometric correction of apparent lengths on projected images is required. In this study, I surveyed Phobos and Gaspra, because I have otherwise been unable to find measured lines that have both sufficient illumination and sufficiently detailed shape models to correct the projected image geometrically. Shape models are commonly given by

Table 1. Specifications of grooves of small irregular bodies.

		Groove Size [m]	
	Size [km]	Length, Width, Depth	Reference
Phobos	13.5 × 10.8 × 9.4	8000, ∼100, 10–20	Thomas *et al.* (1979)
Gaspra	19 × 12 × 11	<1500, ∼100, <20	Veverka *et al.* (1994)
Ida	56 × 24 × 21	<4000, <100, <60	Sullivan *et al.* (1996)
Eros	33 × 13 × 13	<2000, <200, ∼30	Veverka *et al.* (2000)

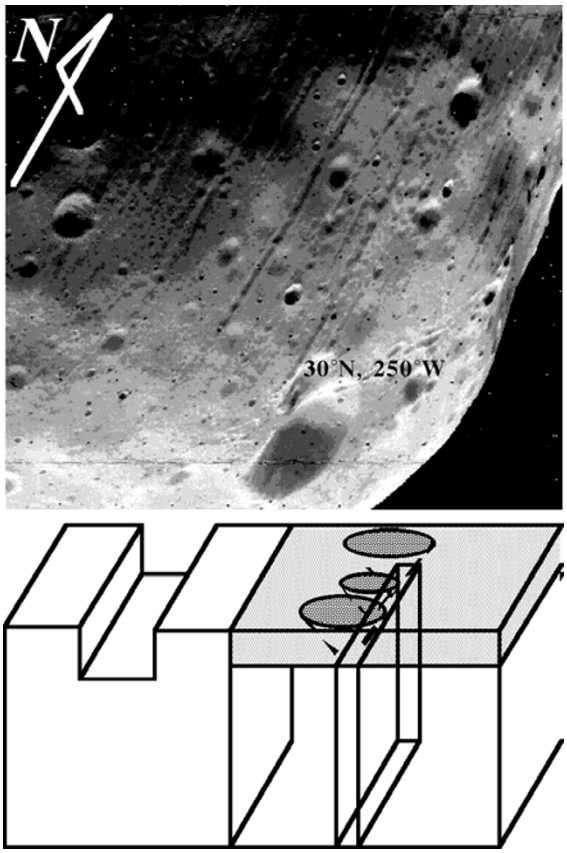

Fig. 1. Appearance of grooves (Phobos). The upper is the grooves from the Stickney crater. The bottom left is an idealized "exposed groove." The bottom right is idealized fissure covered with a regolith layer, and this looks like a chain of cones.

numerical shape models such as those of Simonelli *et al.* (1993) and Thomas (1993). The longest line on a body is a great circle, and the best region for reading a topographic pattern is located along the terminator line. In the case of an image of the subsolar region, with a phase angle of close to zero, any small change in elevation is hard to detect. In view of this restriction in observations and the simplicity of this analysis, I measured a trace of the grooves along a measured line, *not* the size distribution of the length of the grooves.

The areas, lengths, and intervals of fractures are assumed to show a power-law form for the size-frequency distribution. If we assume that all fractures show a similar shape, a specific definition of the size measurements is not required; all size parameters in the same dimension can be converted to each other by means of certain coefficients, but the power-law index is constant. It should be noted that if the extent of each fracture plane is isotropic, the power-law indices for spacing and real size may be interchangeable. The dimensional analysis given below shows that the power-law index of the size-frequency distribution is also easily converted.

The relationships for the 3D size-frequency distribution, 2D trace, and 1D trace of a 2D trace are summarized. These correspond to fracture planes, grooves, and spacing of grooves, respectively. First, the cumulative number of fractures with a characteristic length of fracture, S, is given. The function $D[\ ]$ denotes the dimension of the physical quantity in the parenthesis; L means a dimension of length. The cumulative power-law distribution can be represented as follows:

$$N_S = k_S S^{-\frac{\phi}{2}}, \quad \text{where} \quad D[N_S] = [\#/L^3],$$
$$D[S] = [L], \quad D[k_S] = \left[L^{\frac{\phi-6}{2}}\right].$$

This formulation follows Housen and Holsapple (1999). If ϕ is equal to 6, the factor k_S is a non-dimensional parameter. This condition means that the interval between fractures is equal to the characteristic length of the fractures. Housen and Holsapple (1999) call this the "fully cracked" condition. This is a lower limit on ϕ, because at this value failures are perfectly connected with each other.

Next, the trace of the fractures is considered. The cumulative size distribution of a trace can be parameterized by the characteristic length R, which corresponds to the length of the grooves, as follows:

$$N_R = f(k_S, \phi, R),$$
$$\text{where} \quad D[N_R] = [\#/L^2], \quad D[R] = [L].$$

This size-frequency distribution also shows a power-law distribution, because this operation does not change the original functional form. The left-hand side can be made dimensionless by multiplying by R^2. Then, because the power-law distribution does not show any characteristic scale, the left-hand side of the equation is simply proportional to the function's arguments. The following distribution can therefore be derived:

$$N_R R^2 = f\left(k_S / R^{-\frac{\phi-6}{2}}\right) \propto k_S / R^{\frac{\phi-6}{2}}.$$

This relation can be rearranged to give an equation with another coefficient:

$$N_R \propto k_S R^{1-\frac{\phi}{2}} \equiv k_R R^{1-\frac{\phi}{2}},$$
$$\text{where} \quad D[k_R] = \left[L^{\frac{\phi-6}{2}}\right] = D[k_S].$$

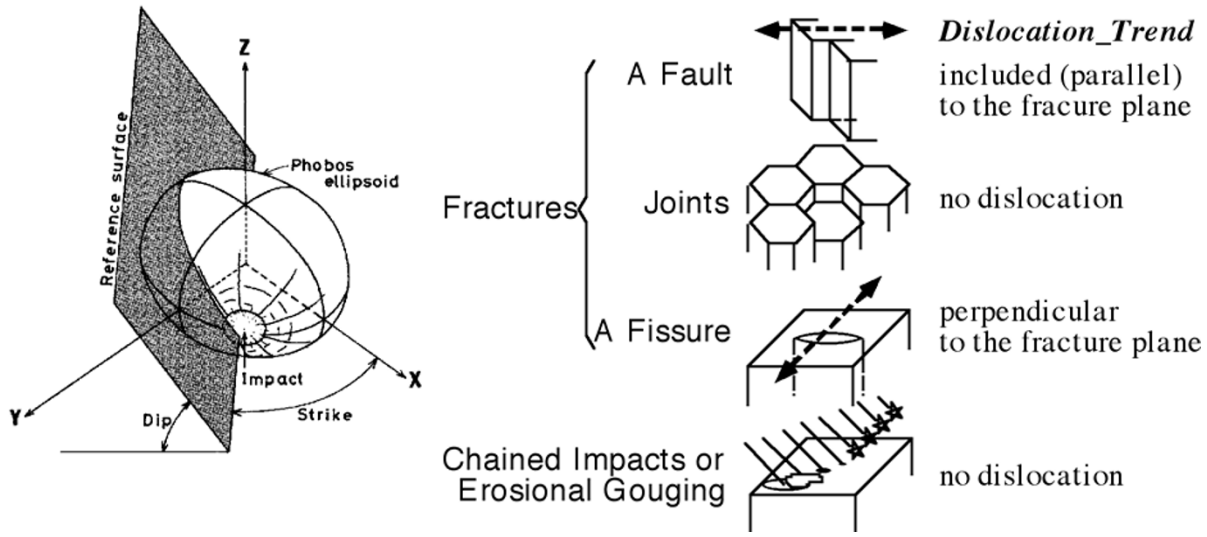

Fig. 2. Origins of grooves. The left shows grooves as outcrops of internal fractures after Kawakami *et al.* (1991). The right shows proposed origins of grooves.

In the same way, a trace of the grooves is derived as follows:

$$N_Q = f(k_R, \phi, R),$$
$$\text{where} \quad D[N_Q] = [\#/L], \quad D[Q] = [L].$$
$$\text{Thus,} \quad N_Q Q^2 = f\left(k_R/Q^{\frac{\phi-6}{2}}\right) \propto k_R/Q^{\frac{\phi-6}{2}},$$
$$N_Q \propto k_R Q^{2-\frac{\phi}{2}} \equiv k_Q Q^{2-\frac{\phi}{2}},$$
$$\text{where} \quad D[k_Q] = \left[L^{\frac{\phi-6}{2}}\right] = D[k_R] = D[k_S].$$

Discrete, counting datasets of this quantity for the two objects studied can then be represented on a log-log plot as a function of length. Although Pickering *et al.* (1995) noted that the biasing effect of truncation is much larger for the left side than the right side of such a plot, I eliminated both terminal values before plotting the data. Moreover, I confirmed that the number of samples was much larger than the number of bits of dynamic range (steps between the maximum and minimum values). The sampling bias is therefore as small as possible in the discussion that follows.

3. Results

The measured values are plotted in Fig. 3. The measured circle on Phobos was the primary meridian (0° and 180° in longitude), and the measured line on Gaspra was from (35°N, 10°W) to (80°N, 190°W). The derived power-law indices were converted to values for the index ϕ of the fracture planes, using the results derived above. Both indices are nearly equal to 6, the fully cracked condition. Phobos's smaller ϕ indicates that Phobos has been more fractured than Gaspra. The two values are as follows:

$$N_S = k_S S^{-\frac{\phi}{2}} \quad \text{for Phobos,} \quad \phi = 5.9;$$
$$\text{for Gaspra,} \quad \phi = 6.5.$$

The data for Phobos can be divided into sufficient intervals for fitting, but not those for Gaspra. Although both sides of a power-law plot are biased by truncation effects (Pickering *et al.*, 1995), the value for Gaspra regressed with all the data points is similar to that obtained when only the central two data points are used (so as to minimize the biasing). Thus, I adopt a value of −1.3 for Gaspra's spacing power-law index. On the other hand, Phobos' regressed value without both terminal data points gives a confidence factor for the regression of close to 1, and I adopt a value of −0.94 for Phobos's spacing power-law index. The good confidence factors for these fits support the hypothesis that the size distributions are power-law in nature.

4. Discussion

Based on the terrestrial database of faults and microcracks, Housen and Holsapple (1999) anticipated that the asteroidal power-law index would be equal to 6, the fully cracked condition. This study supports that expectation, although compressional strength is greater than tensile strength. Fracturing in terrestrial samples is chiefly controlled by compressional strength, whereas in asteroids fracturing caused by impacts would be controlled by tensile strength. However, the result presented here suggests that in asteroids the difference is negligibly small.

In the case of Phobos, parallel grooves along the equator have been reported (e.g., Thomas *et al.*, 1978). This anisotropic distribution of grooves would cause a dependence of the results on the choice of measuring line. Generally traces are blind to direction. If a trace of a 3D body is a plane, the trace cannot detect any planes and lines that are parallel to it. If a trace is an infinite straight line on a sphere, the trace cannot detect any lines and planes that are parallel to the circle, and the result only reflects specific components of the strength. If the trace is a great circle, the detectable components are obvious; Phobos's fully cracked condition reflects only components perpendicular to the measured circle. The terminator is regarded as a great circle of the body, but the limited terminator that was adopted as the measured line for Gaspra might have produced ambiguities in the direction of the specific components of strength measured by these results, because of the irregularity of the body. These

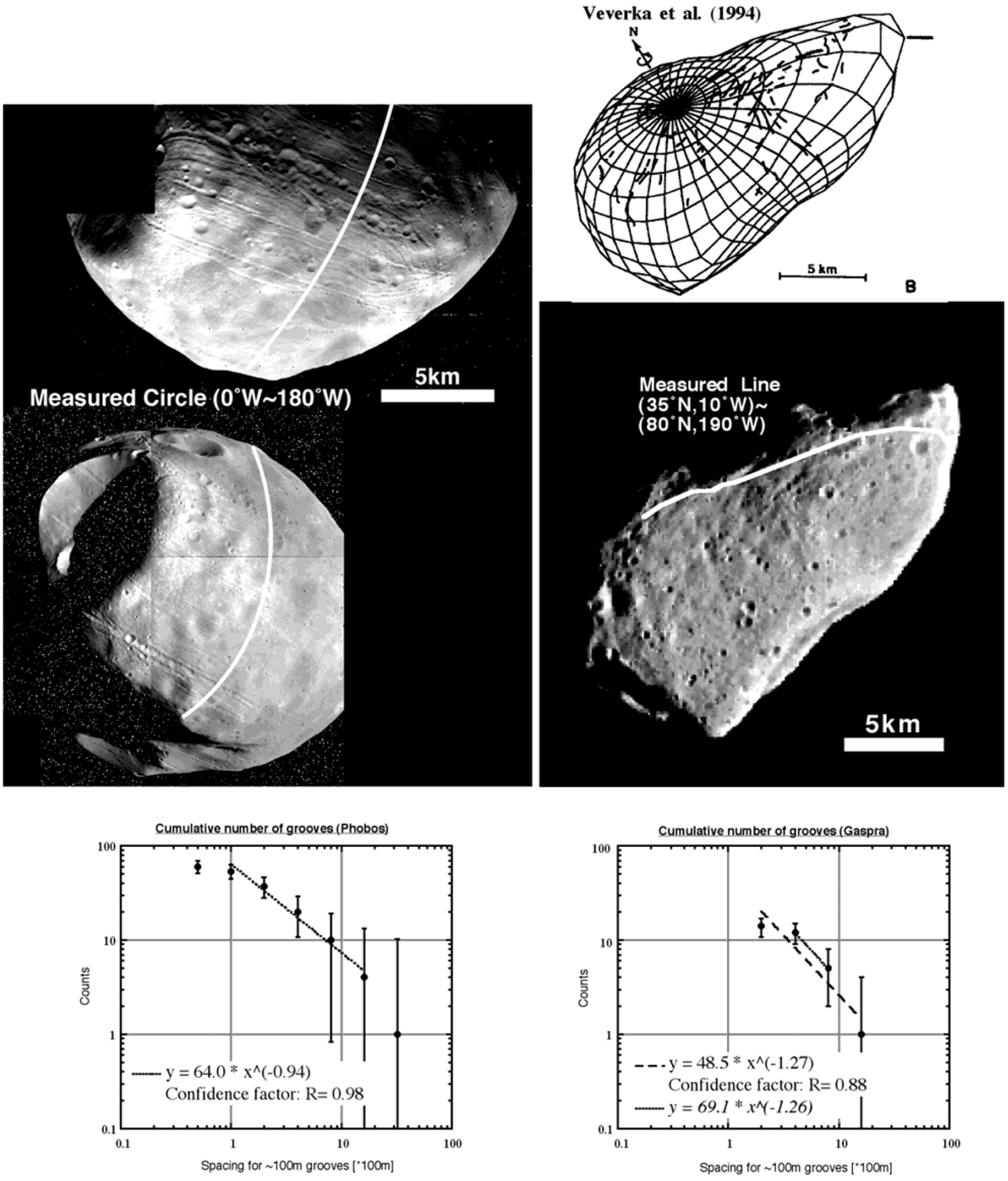

Fig. 3. Cumulative number plots of grooves of Phobos and Gaspra.

results should therefore be applied cautiously.

Generally, strength is defined as a threshold stress or as a specific energy per volume. Housen and Holsapple (1990) and Housen (1991) treated the latter as strength (Q^*), and derived it from a power-law distribution of flaws by dimensional analysis:

$$M_L/M = F[Q^* D^{9\mu/(2\phi-3)} U^{3\mu-2}],$$

where M_L is the largest fragment mass, μ is the coupling parameter, D is the diameter of the target, and U is the impact velocity. In the case of catastrophic impacts that produce a given mass fraction in the largest fragment, the argument of the unknown function $F[\ ]$ on the right-hand side of this equation is constant. A relationship between the strength and the target size can therefore be derived:

$$Q^* \propto D^{-9\mu/(2\phi-3)} \cdot U^{2-3\mu}.$$

In this study, Phobos and Gaspra displayed the fully

cracked condition, with the lowest possible ϕ. The above-stated relationship under these conditions gives rise to the largest possible scaling effect of size on strength. Although recent works on scaling laws have considered this size-dependence factor, the results presented here suggest that typical irregular bodies are in the fully-cracked limit, and therefore have a very strong size-strength dependence. Strengths derived without taking this factor into account are simply ideal values, representing the upper limits of the true strengths. However, in order to verify that such bodies are commonly in the fully cracked condition, further studies of other bodies that exhibit grooves (such as Eros) are required.

5. Summary

The grooves of Phobos and Gaspra follow a similar power-law distribution, close to the theoretical expectation of the fully cracked condition of $\phi \sim 6$ in $N_S = k_S S^{-\frac{\phi}{2}}$, with the caveat that only axial strength was measured by the analysis. This is the lowest possible value of ϕ, implying that the characteristic length of fractures was almost equal to the interval between fractures. This implies that the dependence of mechanical strength on target size is significant. This fully cracked condition may well be common in the solar system, according to the prediction of Housen and Holsapple (1999). If this is the case, asteroids are weaker than previously thought.

Acknowledgments. I would like to acknowledge the continuing guidance and encouragement of Professor Fujiwara and Professor Nakamura. I am also grateful to Dr. Yano for giving me the opportunity to present this paper at the Western Pacific Geophysics Meeting in Tokyo, June 2000. The comments and suggestions of an anonymous reviewer and Dr. Housen were very helpful for improving the manuscript.

References

Fujiwara, A. and N. Asada, Impact fracture patterns on Phobos ellipsoids, *Icarus*, **56**, 590–602, 1983.

Griffith, A. A., The phenomena of rupture and flow in solids, *Philosophical Transaction Royal Society of London Series A*, **34**, 137–154, 1920.

Housen, K. R., Laboratory simulations of large-scale fragmentation events, *Icarus*, **94**, 180–190, 1991.

Housen, K. R. and K. A. Holsapple, On the fragmentation of asteroids and planetary satellites, *Icarus*, **84**, 226–253, 1990.

Housen, K. R. and K. A. Holsapple, Scale effects in strength-dominated collisions of rocky asteroids, *Icarus*, **142**, 21–33, 1999.

Kawakami, S. *et al.*, An experimental study of impact fracturing of small planetary bodies in the solar system with an application to Phobos, *Astronomy and Astrophysics*, **241**, 233–242, 1991.

Pickering, G. *et al.*, Sampling power-law distributions, *Tectonophys.*, **248**, 1–20, 1995.

Simonelli, D. P. *et al.*, The generation and use of numerical shape models for irregular Solar System objects, *Icarus*, **103**, 49–61, 1993.

Soter, S. and A. Harris, Are striations on Phobos evidence for tidal stress?, *Nature*, **268**, 421–422, 1977.

Sullivan, R. *et al.*, Geology of 243 Ida, *Icarus*, **120**, 119–139, 1996.

Thomas, P. C., Gravity, tides, and topography on small satellites and asteroids: application to surface features of the Martian satellites, *Icarus*, **105**, 326–344, 1993.

Thomas, P. C. *et al.*, Origin of the grooves on Phobos, *Nature*, **273**, 282–284, 1978.

Thomas, P. C. *et al.*, Grooves on Phobos—Their distribution, morphology and possible origin, *J. Geophys. Res.*, **84**, 8457–8477, 1979.

Veverka, J. and T. C. Duxbury, Viking observations of Phobos and Deimos—Preliminary results, *J. Geophys. Res.*, **82**, 4213–4223, 1977.

Veverka, J. *et al.*, Discovery of grooves on Gaspra, *Icarus*, **107**, 72–83, 1994.

Veverka, J. *et al.*, NEAR at Eros: Imaging and spectral results, *Science*, **289**, 2088–2097, 2000.

H. Demura (e-mail: demura.hirohide@nasda.go.jp)